The Microwave Spectrum of Isopropyl Iodide: The Iodine Hyperfine Structure and a Centrifugal Distortion Analysis

Joachim Gripp and Helmut Dreizler

Abteilung Chemische Physik im Institut für Physikalische Chemie der Universität Kiel

Z. Naturforsch. **45a**, 715–723 (1990); received January 31, 1990

The ground state microwave spectrum of isopropyl iodide has been investigated by microwave Fourier transform (MWFT) spectroscopy. 212 hyperfine components of 39 mainly *a*-type transitions have been assigned from the measured spectra in the frequency range between 4 and 30 GHz. With a MWFT double resonance modulation (MWFTDR) spectrometer a weak *c*-type transition and a "forbidden" $\Delta J = 2$ line could be observed. The spectra were analysed using a diagonalization procedure of the complete Hamiltonian matrix and a simultaneous least squares fit of the rotational, quartic centrifugal distortion and the iodine quadrupole and spin rotation coupling constants directly to the measured frequencies. A set of 14 constants could be obtained with high accuracy. The rotational constant A' and some of the centrifugal distortion constants could be improved using some large higher order quadrupole perturbations and the results of the MWFTDR measurements for the analysis.

Introduction

The microwave spectra of molecules containing an iodine atom show some wide and overlapping hyperfine splittings caused by the large quadrupole coupling of the nuclear spin of iodine and the molecular rotation. In most cases the iodine hyperfine structure is perturbed by higher order effects which can be strong for asymmetric top molecules. The best way of analyzing this kind of spectra is the diagonalization of the complete Hamiltonian matrix combined with a simultaneous least squares fit of all relevant spectroscopic constants directly to the measured frequencies. Then these constants can be determined with the highest possible precision. Gerry and Coworkers [1, 2] have reported that the inclusion of strong higher order quadrupole perturbations additionally could improve the values of rotational and centrifugal distortion constants in the cases of iodine isocyanate and vinyl iodide using this analyzing method. But the procedure has the disadvantage of consuming a lot of computer time and storage capacity.

The microwave spectrum of isopropyl iodide, CH_3CHICH_3, contains some stronger higher order quadrupole perturbations. So we thought the spectrum of this molecule could be a good example for testing the mentioned analyzing method with our program HFS [3] using the Cray XMP 216 vector processor system of the University of Kiel.

The first investigation of the microwave spectrum of isopropyl iodide was reported by Groner et al. [4]. A substitution structure was determined by Ikeda et al. from the microwave spectra of eight isotopic species [5]. Isopropyl iodide is a near prolate asymmetric top molecule with a C_s-point symmetry. The symmetry plane contains the *a* and the *c* principal inertia axes. Reasonably *a*- and *c*-type transitions can be expected, but in [4] and [5] only the observation of *a*-type transitions is reported because the *c*-type transitions are very weak. With the normal MWFT method we too could observe only *a*-type transitions, but we were able to assign the *c*-type transition $J' K'_- K'_+ - J K_- K_+ = 313 - 303$ with one of our MWFTDR spectrometers [6]. Furthermore, the observation of a "forbidden" $\Delta J = 2$ *c*-type line caused by an extremely strong higher order quadrupole perturbation was possible using this method. Additionally some *a*-type transitions being affected by this perturbation have been measured with the normal MWFT method. We will show that the inclusion of these transitions in the analysis of the spectrum could improve the values of the rotational constant A' and some of the quartic centrifugal distortion constants. They are otherwise not very well determined using more weakly perturbed *a*-type transitions only. Due to the high accuracy of the MWFT measurements the iodine spin-rotation coupling had to be considered for the analysis like in similar cases [7, 8].

Reprint requests to Prof. Dr. H. Dreizler, Abteilung Chemische Physik im Institut für Physikalische Chemie Kiel, Olshausenstr. 40, D-2300 Kiel, FRG.

0932-0784 / 90 / 0500-0715 $ 01.30/0. – Please order a reprint rather than making your own copy.

Dieses Werk wurde im Jahr 2013 vom Verlag Zeitschrift für Naturforschung in Zusammenarbeit mit der Max-Planck-Gesellschaft zur Förderung der Wissenschaften e.V. digitalisiert und unter folgender Lizenz veröffentlicht: Creative Commons Namensnennung-Keine Bearbeitung 3.0 Deutschland Lizenz.

This work has been digitalized and published in 2013 by Verlag Zeitschrift für Naturforschung in cooperation with the Max Planck Society for the Advancement of Science under a Creative Commons Attribution-NoDerivs 3.0 Germany License.

Zum 01.01.2015 ist eine Anpassung der Lizenzbedingungen (Entfall der Creative Commons Lizenzbedingung „Keine Bearbeitung") beabsichtigt, um eine Nachnutzung auch im Rahmen zukünftiger wissenschaftlicher Nutzungsformen zu ermöglichen.

On 01.01.2015 it is planned to change the License Conditions (the removal of the Creative Commons License condition "no derivative works"). This is to allow reuse in the area of future scientific usage.

Experimental

The spectra were recorded with our MWFT spectrometers between 4 and 30 GHz [9–15]. The MWFTDR measurements were made with our spectrometers described in [6]. The sample of isopropyl iodide was obtained commercially and used without further purification. The measurements were carried out at pressures between 0.3 and 2.5 mTorr (0.04 and 0.33 Pa) and temperatures between $-20°$ and $-40°$ C.

The Attributes of Higher Order Quadrupole Perturbations

In case of large hyperfine splittings as caused by the quadrupole coupling of the iodine nucleus in the rotational spectra of iodine containing compounds, higher order perturbations may be present. They can be used not only for the determination of the off diagonal components of the quadrupole coupling tensor but also for an indirect determination of the rotational and centrifugal distortion constants in the cases of asymmetric top molecules. This can be expressed approximately using a perturbation formula up to second order for the quadrupole interaction similar to that given by Gordy [16]:

$$E_Q = \langle \tau, J, I, F, M_F | \hat{H}_Q | \tau, J, I, F, M_F \rangle + \sum_{J', \tau' \neq J, \tau} \frac{|\langle \tau', J', I, F, M_F | \hat{H}_Q | \tau, J, I, F, M_F \rangle|^2}{E_{J\tau} - E_{J'\tau'}}. \quad (1)$$

The matrix elements have been set up in a coupled basis consisting of the eigenfunctions of the rotational Hamiltonian and the spin functions due to the coupling nucleus. In the cases of asymmetric top molecules, τ represents the pseudo quantum numbers K_- and K_+ of the limiting prolate and oblate symmetric tops. The first term contains a diagonal matrix element of the quadrupole interaction Hamiltonian $\hat{H}_Q$ and is equivalent to the first order perturbation. The second order perturbation is given by the sum over the squares of absolute values of the off diagonal matrix elements of $\hat{H}_Q$ divided by the difference of the corresponding unperturbed rotational energies. These unperturbed levels only are influenced by the rotation and centrifugal distortion contributions in a first order approximation.

So it can be seen that for the first order perturbation no dependence of the unperturbed rotational levels is given while the second order contribution contains information about level differences and can be used for their determination. This may be valuable if level differences cannot be obtained spectroscopically.

The existence of the matrix elements in (1) can be determined using their symmetry properties. The elements vanish if the direct product of the irreducible representations of the symmetry group reflecting the transformation properties of the basis functions and the operator does not contain the total symmetric representation A of the group. The matrix elements of $\hat{H}_Q$ may be decomposed in the following way:

$$\langle \tau', J', I, F, M_F | \hat{H}_Q | \tau, J, I, F, M_F \rangle = (-1)^{J+I+F} \cdot \begin{Bmatrix} F & I & J' \\ 2 & J & I \end{Bmatrix} \begin{pmatrix} I & 2 & I \\ -I & 0 & I \end{pmatrix}^{-1} \begin{pmatrix} J & 2 & J' \\ J & 0 & -J \end{pmatrix}^{-1} \cdot \langle \tau', J', M_J' = J | \hat{V}_{ZZ} | \tau, J, M_J = J \rangle \cdot eQ/4, \quad (2)$$

where $\hat{V}_{ZZ}$ is one component of the field gradient tensor referred to space fixed cartesian axes, Q represents the nuclear quadrupole moment and e is the elementary charge. The parentheses denote Wigner $3j$-symbols and the curled brackets Wigner $6j$-symbols [17]. It can be proved that for asymmetric tops the basis functions in (1) transform according to the irreducible representations of the group $D_2 \equiv V$ like the eigenfunctions of an unperturbed asymmetric top. These transformation properties are not affected by the quantum numbers F, I and J, as follows from the features of the $3j$- and $6j$-symbols in (2). A more detailed description is given in [18]. The irreducible representations A, B_a, B_b, and B_c of the group D_2 can be assigned to the basis functions of (1) by the parity of their pseudo quantum numbers K_- and K_+ as in the case of the unperturbed asymmetric top eigenfunctions [19]:

$$\begin{aligned} |\mathrm{e,e}\rangle &\triangleq A, \quad |\mathrm{e,o}\rangle \triangleq B_a, \\ |\mathrm{o,o}\rangle &\triangleq B_b, \quad |\mathrm{o,e}\rangle \triangleq B_c. \end{aligned} \quad (3)$$

e = even and o = odd represent the parities of K_- and K_+. The other quantum numbers have been omitted for simplicity.

The $\hat{V}_{ZZ}$ containing matrix elements will be transformed to the principal inertia axes a, b, and c using the direction cosine matrix elements in the asymmetric

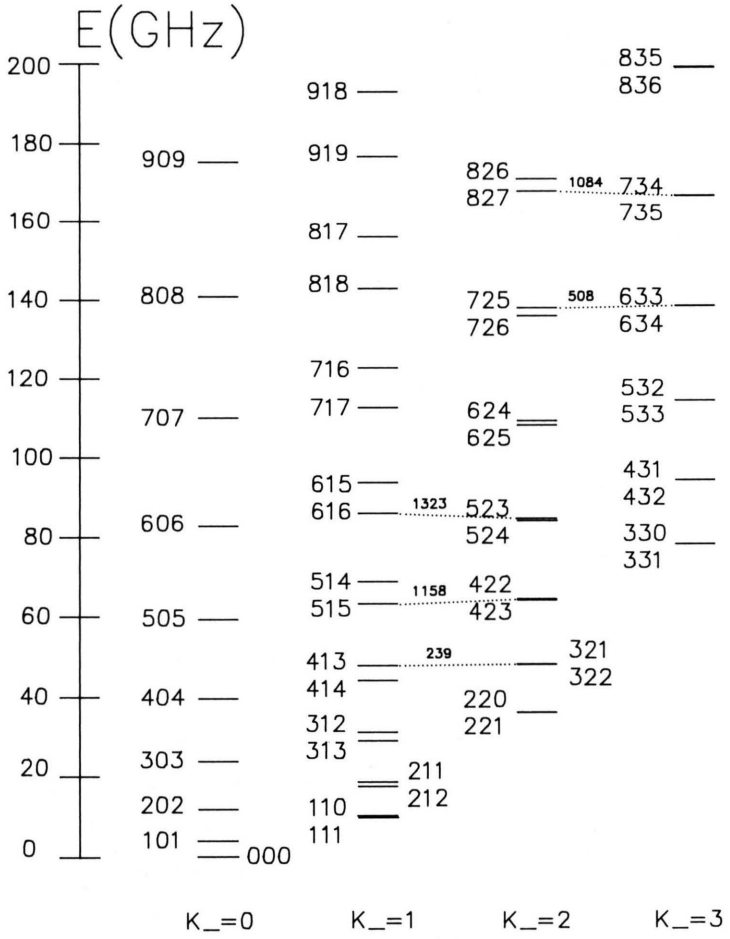

Fig. 1. The rotational energy levels of isopropyl iodide labelled with the quantum numbers JK_-K_+ and arranged in the order of K_- up to 200 GHz. The dotted lines connect levels which are strongly perturbed by matrix elements containing the off diagonal component χ_{ac} of the quadrupole coupling tensor. The level differences are given in MHz.

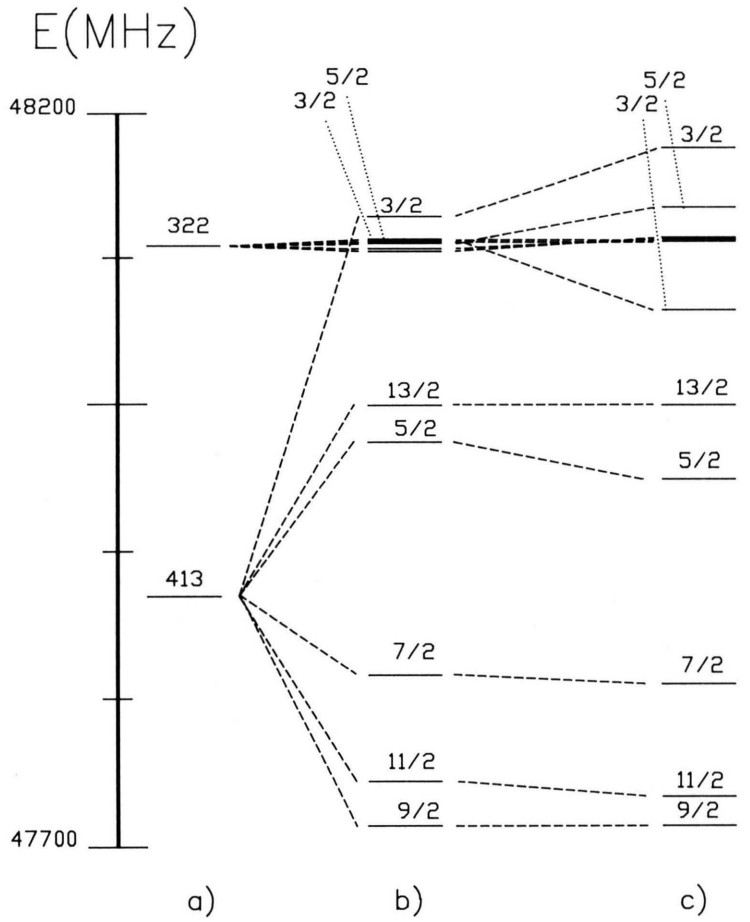

Fig. 2. A detailed energy level diagram of the most strongly perturbed rotational level pair $JK_-K_+ = 322$ and 413 of isopropyl iodide labelled with the JK_-K_+ and F quantum numbers. a) Rotational energies; b), c) hyperfine splitting calculated without b) and with c) the influence of χ_{ac}. For the rotational level $JK_-K_+ = 322$ only the sublevels with the quantum numbers $F = 3/2$ and 5/2 are marked for simplification.

rotor basis:

$$\langle K'_-, K'_+, J', M'_J = J \mid \hat{V}_{ZZ} \mid K_-, K_+, J, M_J = J \rangle$$

$$= \sum_{g,g'=a,b,c} \langle K'_-, K'_+, J', M'_J = J \mid (\hat{\Phi}_{Zg}\, \hat{\Phi}_{Zg'}) \mid K_-, K_+, J, M_J = J \rangle \cdot V_{gg'} \,. \tag{4}$$

The $eQV_{gg'} = \chi_{gg'}$ are the spectroscopically determinable constants of the quadrupole coupling tensor in the principal inertia axes system. The direction cosines also transform according to the irreducible representations of the group D_2, as has been mentioned by Gordy [20]:

$$\hat{\Phi}^2_{Za}, \hat{\Phi}^2_{Zb}, \hat{\Phi}^2_{Zc} \triangleq A, \quad \hat{\Phi}_{Za}, \hat{\Phi}_{Zb}\, \hat{\Phi}_{Zc} \triangleq B_a,$$
$$\hat{\Phi}_{Zb}, \hat{\Phi}_{Zc}\, \hat{\Phi}_{Za} \triangleq B_b, \quad \hat{\Phi}_{Zc}, \hat{\Phi}_{Za}\, \hat{\Phi}_{Zb} \triangleq B_c \,. \tag{5}$$

In conclusion we obtain the nonvanishing matrix elements containing components of the quadrupole coupling tensor by calculating the direct products of the irreducible representations.

The matrix elements of $\hat{H}_Q$ are finally obtained by inserting these results in (1) and (2). It follows that the diagonal elements of $\hat{H}_Q$, and consequently the first order contributions, arise only from the diagonal components χ_{gg} of the quadrupole coupling tensor. The second order contributions of the χ_{gg} resulting from their matrix elements off diagonal in J but diagonal in K_- and K_+ are small in general because they connect widely separated unperturbed levels in most cases. The off diagonal components $\chi_{gg'}$ contribute only to the second order perturbations because all their diagonal matrix elements vanish. But their off diagonal matrix elements may connect closely spaced or near degenerate levels, and then large perturbations can be noticed.

In Fig. 1 the rotational energy diagram of isopropyl iodide is given. Strong second order perturbations arising from the connection of two rotational levels by χ_{ac} containing matrix elements are indicated. The perturbing connections are restricted to a pair of levels with both pseudo quantum numbers K_- and K_+ changing parity. For isopropyl iodide the off diagonal components χ_{ab} and χ_{bc} vanish by the molecular symmetry.

The most important second order perturbation in the spectra of isopropyl iodide arises between the rotational levels with the quantum numbers $J K_- K_+ = 322$ and 413. These levels are separated by a difference of only 239 MHz. A detailed energy diagram containing the hyperfine splittings is displayed in Figure 2. The sublevels with the quantum number $F = 3/2$ are closely spaced and inverted relative to the rotational levels in this case. The inclusion of χ_{ac} containing matrix elements repell both sublevels by an amount of approximately 50 MHz.

Higher order perturbations of this strength can only be treated satisfactorily using diagonalization procedures, but transitions containing them give the most valuable information about the difference of the perturbed levels and the off diagonal components of the quadrupole coupling tensor. They also have a remarkable influence on the line intensity caused by mixing of the wave functions of the perturbed levels. Reasonably "forbidden" transitions can be observed in some cases.

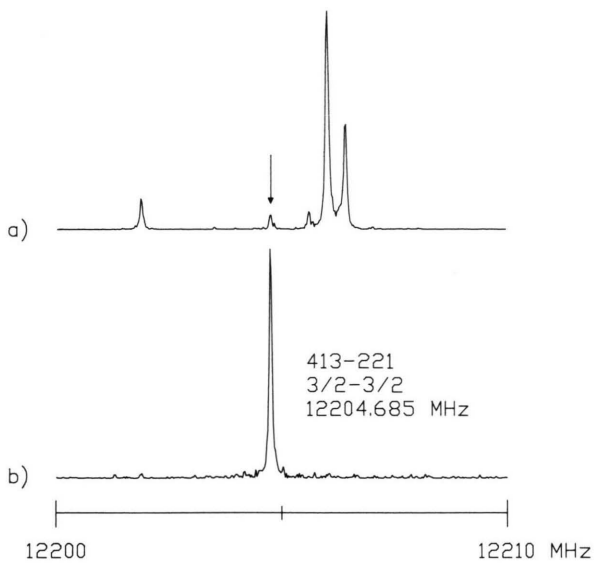

Fig. 3. The "forbidden" line $J' K'_- K'_+ - J K_- K_+ = 413 - 221$, $F' - F = 3/2 - 3/2$ of isopropyl iodide. a) Normal MWFT record. Experimental conditions: power spectrum, $4.9 \cdot 10^6$ averaging cycles, sample interval: 10 ns, 2048 data points supplemented with 2048 zeros before Fourier transformation, pressure: ≈ 2.5 mTorr (0.33 Pa), temperature: ≈ -20 °C, polarizing frequency: 12 204.988 MHz. b) Recorded with double resonance modulation. Experimental conditions: $8.2 \cdot 10^6$ averaging cycles, other conditions see a). The hyperfine component $J' K'_- K'_+ - J K_- K_+ = 514 - 413$, $F' - F = 5/2 - 3/2$ at 20 816.692 MHz has been used as a pump transition.

We succeeded in the observation of the hyperfine component $F'-F=3/2-3/2$ of the "forbidden" c-type rotational transition $J'K'_-K'_+-JK_-K_+=413-221$ using the MWFTDR method (Figure 3). The a-type component $J'K'_-K'_+-JK_-K_+=514-413$, $F'-F=5/2-3/2$ has been used for the DR pump modulation. In a second experiment, for comparison the corresponding a-type component $J'K'_-K'_+-JK_-K_+=322-221$, $F'-F=3/2-3/2$ was observed and the "forbidden" c-type component $J'K'_-K'_+-JK_-K_+=514-322$, $F'-F=5/2-3/2$ has been taken for the pump transition.

Ikeda et al. [5] have reported some hyperfine components of the "forbidden" c-type transition $J'K'_-K'_+-JK_-K_+=514-322$ in the spectrum of the deuterated species CH_3CDICH_3. In this case the hyperfine levels with $F=11/2$, $9/2$ and $7/2$ are strongly perturbed while the perturbation of the $F=3/2$ level is much weaker.

Analysis and Results

A total of 212 hyperfine components of 39 rotational transitions of isopropyl iodide up to $J=20$ has been assigned from the measured spectra. The major part of the measurements could be directly used for the analysis. In case of narrow splittings a line shape analysis for the correction of frequencies was necessary [21]. No splittings due to the internal rotation of the methyl groups could be observed because of the high hindering barrier. The spectroscopic constants have been evaluated by a simultaneous least squares fit directly to the obtained frequencies using a diagonalization procedure of the complete Hamiltonian matrix for the calculation of the eigenvalues. For the centrifugal distortion contribution the Hamiltonian of Van Eijck and Typke has been used [22, 23], and all quartic constants could be determined. Attempts to obtain the sextic constants did not improve the fit, and most of them were indeterminable. So they were neglected in the final calculations. In Table 1 the observed and calculated frequencies and the assignments are given. As in the case of ethyl iodide [8], the consideration of the iodine spin rotation coupling allowed the determination of these constants and the improvement of the others. The deviations between observed and calculated frequencies are then below 10 kHz and reproduce approximately the accuracy of our measurements.

Table 2 contains the results of two calculations with (Table 2a) and without (Table 2b) inclusion of the spin rotation coupling contribution. All constants of Table 2a are well determined with a total standard deviation being only 3.3 kHz. The constant χ_{ac} is nearly as well determined as the diagonal components of the quadrupole coupling tensor because of the many higher order perturbations used in the analysis. The neglection of the spin rotation coupling (Table 2b) leads to increasing errors of all constants, but its influence in the spectrum of isopropyl iodide is smaller than in case of ethyl iodide. A possible reason may be the larger moments of inertia and therefore the smaller angular velocity of isopropyl iodide relative to ethyl iodide.

In addition, the components of the quadrupole coupling tensor in its own principal axes system (x', y', z') have been obtained by diagonalization [24]. The z'-axis of the tensor and the C–I bond axis form an angle of approximately 1°. The z'-axis inclines toward the hydrogen atom of the CHI group as has been reported by Ikeda et al. [5].

We were particularly interested in the improvement of the rotational constant A' and some of the centrifugal distortion constants (especially D'_K) by the MWFTDR measurements and the lines being influenced by the very strong quadrupole perturbations of the levels $JK_-K_+=322$ and 413. So we performed three other calculations. Their results are given in Table 3. In the first calculation (Table 3a) all MWFTDR measurements have not been considered. The results are of similar quality as those of Table 2a although only a-type transitions have been used. In the second calculation (Table 3b) the a-type hyperfine components containing one of the most strongly perturbed levels $JK_-K_+=322$ and 413, $F=3/2$ and $5/2$ have been additionally neglected. In this case the determination errors of the constants A', D'_K, δ'_J and R'_6 and particularly the correlation coefficients among these constants increase because now these constants can no longer be separated completely. In addition the error of the quadrupole coupling constant χ_{ac} increases. The inclusion of the c-type transition $J'K'_-K'_+-JK_-K_+=313-303$, while excluding the strongly perturbed hyperfine components for a second time, leads again to a satisfying separation of the mentioned constants (Table 3c). So we think that for the improvement of the mentioned rotational and centrifugal distortion constants the contributions from the weak c-type transitions and the most strongly

Table 1. Observed and calculated frequencies of CH_3CHICH_3. ν: measured frequency (MHz), $\bar{\nu}$: hypothetical unsplit center frequency (MHz), δ_{tot}: observed minus calculated frequencies using the constants of Table 2a (kHz), δ_{NQ}: observed minus calculated frequencies using the constants of Table 2b (spin rotation contribution neglected, kHz). The quantum numbers of the most strongly perturbed hyperfine levels are marked with an asterisk.

$J'K'_-K'_+ - JK_-K_+$	$2F'-2F$	ν	δ_{tot}	δ_{NQ}
$\bar{\nu}$				
a-type transitions				
1 0 1 0 0 0	7 5	4 090.161	−1.5	17.0
4 004.851	3 5	4 238.925	−0.6	−26.1
2 0 2 1 0 1	9 7	8 028.648	2.1	22.6
7 992.696	7 5	8 060.545	1.5	14.8
	7 7	7 719.394	3.3	−4.6
	5 3	7 659.457	6.3	16.7
	3 3	7 887.075	1.8	−7.8
2 1 1 1 1 0	9 7	8 483.812	0.4	22.2
8 379.211	7 7	8 320.897	−6.0	−12.7
	5 5	8 201.861	−1.2	−10.2
	7 5	8 160.363	−7.0	7.2
2 1 2 1 1 1	9 7	7 742.938	−3.0	18.1
7 640.154	7 5	7 419.336	−7.3	6.3
	5 5	7 452.320	0.1	−8.8
3 0 3 2 0 2	11 9	11 966.004	0.5	22.4
11 946.753	9 7	11 981.216	−3.7	11.0
	7 7	11 984.923	1.6	−15.4
	7 5	11 896.103	4.9	13.5
	5 3	11 819.251	3.4	5.8
3 1 2 2 1 1	9 7	12 533.099	0.2	15.5
12 557.912	7 7	12 534.689	0.0	−15.7
	9 9	12 370.187	−2.1	−15.4
	7 9	12 371.778	−2.1	−46.3
	5 7	12 655.104	4.9	−35.8
3 1 3 2 1 2	11 9	11 494.370	−0.6	21.6
11 449.824	7 5	11 388.956	1.6	9.3
	5 3	11 383.037	−0.2	0.2
	9 7	11 421.722	−1.8	13.1
3 2 1 2 2 0	11 9	12 201.827	0.1	24.0
12 082.237	9 7	11 888.796	0.8	16.3
	7 7	11 883.127	7.3	−3.3
	7 5	11 968.265	2.0	6.4
	5 5	11 973.547	5.3	−10.8
3 2 2 2 2 1	11 9	12 142.166	2.6	26.8
12 014.473	9 9	12 140.558	−3.2	−11.6
	9 7	11 822.007	3.6	19.1
	7 5	11 907.231	0.2	4.8
	5* 3	12 163.139	0.2	−6.5
	3* 3	12 092.714	2.9	−19.5
4 0 4 3 0 3	13 11	15 862.932	−1.2	21.1
15 851.434	11 9	15 874.384	−0.7	14.6
	9 9	15 842.604	4.5	−18.5
	9 7	15 838.899	0.5	9.3
	7 5	15 801.029	−0.4	1.8
	5 3	15 788.319	1.0	−3.7
	11 11	15 580.351	4.8	−15.4
4 1 3 3 1 2	13 11	16 747.986	−0.4	22.8
16 722.825	11 9	16 716.562	−3.1	12.2
	11 11	16 482.743	−2.0	−22.7
	9 7	16 695.399	0.3	8.9
	9 9	16 696.989	−0.2	−22.6
	7 5	16 670.913	0.7	1.8
	5* 3	16 659.534	2.0	−4.4
	3* 1	16 771.756	4.0	−8.9
4 1 4 3 1 3	13 11	15 271.844	0.3	22.9
15 247.671	11 9	15 248.042	−1.3	14.1
	9 7	15 221.425	−9.1	−0.6
	9 9	15 221.638	−2.7	−24.0
	7 5	15 205.143	−1.3	0.3
	5 3	15 213.611	2.5	−3.1
	11 11	15 041.671	2.1	−16.1
4 2 2 3 2 1	13 11	16 237.266	1.1	25.0
16 173.880	11 9	16 114.742	0.3	16.2
	11 11	16 119.297	−5.1	−21.4
	9 9	16 099.006	−1.2	−20.0
	9 7	16 104.683	0.1	7.3
	5 3	16 220.958	−2.0	−11.6
	3 1	16 291.473	−5.5	−23.1
	3 3	16 291.066	4.3	−21.9
4 2 3 3 2 2	13 11	16 055.904	−3.8	19.3
16 006.020	11 11	15 946.022	−4.3	−21.1
	11 9	15 947.629	0.9	16.7
	9 9	15 931.480	−5.9	−24.6
	9 7	15 931.454	1.8	9.0
	7 5*	15 954.868	0.4	−1.1
	5 3*	16 097.821	−3.4	−12.0
4 3 1 3 3 0	13 11	16 173.747	9.2	33.8
16 054.685	11 9	15 904.062	−1.8	14.0
	9 7	15 913.448	−3.9	1.3
	7 5	16 066.169	0.2	−5.7
	5 3	16 242.967	1.9	−14.1
4 3 2 3 3 1	13 11	16 170.719	5.9	30.5
16 051.754	11 9	15 901.088	−2.7	13.0
	9 7	15 910.513	7.4	12.6
	7 5	16 063.236	0.7	−5.2
	5 3	16 240.025	−0.5	−16.4
5 1 4 5 1 5	13 13	5 521.141	−2.8	−2.1
5 529.175	11 11	5 513.904	0.9	−0.2
	9 9	5 522.594	−0.4	−2.6
	7 7	5 539.328	−1.2	−4.0
	5 5	5 555.736	3.8	0.6
6 1 5 6 1 6	17 17	7 733.047	0.9	5.1
7 719.082	15 15	7 706.806	−3.1	−1.7
	13 13	7 703.546	−1.8	−2.5
	11 11	7 709.746	1.2	−0.9
	9 9	7 722.155	2.7	−0.4
	7 7	7 738.991	−3.8	−7.4
6 4 2 5 4 1	17 15	24 158.049	−1.0	19.8
24 086.488	15 13	24 027.160	−5.0	7.2
	13 11	24 004.978	−4.7	−1.6
	11 9	24 049.279	−4.6	−10.8
	9 7	24 127.115	−3.9	−19.2
	7 5	24 212.233	−1.1	−24.9
6 4 3 5 4 2	17 15	24 157.630	3.6	24.5
24 086.073	15 13	24 026.747	−1.7	10.6
	13 11	24 004.565	−2.5	0.6
	11 9	24 048.868	−0.4	−6.7
	9 7	24 126.699	−0.7	−16.0
	7 5	24 211.811	4.7	−19.1
7 1 6 7 1 7	19 19	10 259.058	2.6	7.9
10 245.039	17 17	10 235.381	−4.4	−2.3
	13 13	10 235.510	1.8	0.0
	15 15	10 230.050	1.1	1.0
	11 11	10 247.966	−4.4	−7.3
	9 9	10 264.863	3.4	−0.3
7 2 5 6 2 4	19 17	28 770.571	−0.1	20.1
28 753.084	17 15	28 746.017	−4.8	7.2
	15 13	28 738.322	−3.9	0.9
	13 11	28 735.529	3.0	0.2
	11 9	28 739.044	−3.1	−13.8
	9 7	28 755.956	2.3	−16.4

Table 1 (continued)

$J'K'_-K'_+ - JK_-K_+$	$2F'-2F$	ν	δ_{tot}	δ_{NQ}
$\bar{\nu}$				
7 3 4 6 3 3	17 15	28 190.410	−0.2	10.8
28 205.881	15 13	28 175.840	4.3	7.3
	13 11	28 179.914	−4.2	−9.1
7 3 5 6 3 4	19 17	28 168.228	1.4	19.7
28 145.346	17 15	28 129.964	0.0	10.9
	15 13	28 115.123	4.2	7.2
	13 11	28 115.902	−1.1	−6.5
	11 9	28 134.980	3.0	−10.6
	9 7	28 182.020	1.3	−19.1
7 4 3 6 4 2	19 17	28 166.652	6.2	23.7
23 118.478	17 15	28 086.539	2.1	11.4
	15 13	28 067.089	−4.4	−3.6
	13 11	28 087.839	−2.6	−10.3
	11 9	28 133.167	2.8	−13.6
7 4 4 6 4 3	19 17	28 165.177	1.3	18.8
28 117.083	17 15	28 085.022	1.8	11.0
	15 13	28 065.558	2.7	3.4
	13 11	28 086.293	−0.2	−8.0
	11 9	28 131.773	−1.4	−17.8
8 1 7 8 1 8	21 21	13 095.317	4.4	11.0
13 081.508	19 19	13 072.993	−1.0	2.3
	17 17	13 067.056	−1.9	−1.1
	15 15	13 071.714	−0.6	−1.6
	13 13	13 083.598	−1.0	−3.4
	11 11	13 100.304	5.4	2.0
9 1 8 9 1 9	23 23	16 205.538	1.1	9.4
16.192.214	21 21	16 184.551	−1.1	3.8
	19 19	16 178.539	1.7	3.9
	17 17	16 182.511	−2.8	−2.6
	15 15	16 193.562	−0.6	−1.9
	13 13	16 209.664	0.9	−1.6
10 2 8 10 2 9	25 25	6 737.391	−1.5	3.5
6 725.191	23 23	6 718.791	−0.3	2.2
	21 21	6 712.964	0.8	1.3
	19 19	6 716.249	−1.1	−2.3
	17 17	6 726.176	−1.3	−3.8
	15 15	6 740.855	0.9	−2.7
11 2 9 11 2 10	27 27	9 090.501	−1.5	4.3
9 077.515	25 25	9 071.137	1.8	4.8
	23 23	9 064.694	−2.2	−1.6
	21 21	9 067.856	0.5	−0.9
	19 19	9 078.222	3.2	0.2
	17 17	9 093.900	−1.5	−5.8
12 2 10 12 2 11	29 29	11 815.906	−1.7	4.7
11 802.455	27 27	11 796.164	−0.7	2.5
	25 25	11 789.320	2.1	2.7
	23 23	11 792.296	1.9	0.3
	21 21	11 802.838	−0.3	−3.8
	19 19	11 819.161	−3.6	−8.7
13 2 11 13 2 12	31 31	14 887.687	−1.0	5.8
14 874.136	29 29	14 867.980	2.6	6.1
	27 27	14 860.934	0.5	1.1
	25 25	14 863.671	2.3	0.4
	23 23	14 874.150	−1.4	−5.3
	21 21	14 890.811	−2.3	−8.0
15 3 12 15 3 13	35 35	6 762.248	−1.8	3.4
6 752.539	33 33	6 748.563	0.8	3.7
	31 31	6 743.410	4.1	4.8
	29 29	6 745.120	2.7	1.7
	27 27	6 752.372	0.5	−2.2
	25 25	6 764.065	−2.8	−6.8
16 3 13 16 3 14	37 37	9 116.887	−4.3	1.8
9 106.042	35 35	9 101.747	0.5	3.9
	33 33	9 095.921	1.5	2.4
	31 31	9 097.709	5.6	4.3
	29 29	9 105.717	0.4	−2.7
	27 27	9 118.793	−4.3	−9.1
17 3 14 17 3 15	39 39	11 894.312	−3.6	3.0
11 882.567	37 37	11 878.045	0.7	4.2
	35 35	11 871.685	3.8	4.5
	33 33	11 873.497	2.6	0.7
	31 31	11 882.079	1.0	−3.1
	29 29	11 896.244	−5.5	−11.5
18 3 15 18 3 16	41 41	15 075.094	−7.1	−0.5
15 062.711	39 39	15 058.044	2.8	5.8
	37 37	15 051.302	4.0	3.9
	35 35	15 053.109	4.5	1.6
	33 33	15 062.057	1.2	−4.2
	31 31	15 076.988	−5.2	−12.9
20 4 16 20 4 17	45 45	6 156.133	−3.7	2.0
6 148.722	43 43	6 146.081	1.3	4.8
	41 41	6 141.986	2.1	3.8
	39 39	6 142.955	4.4	4.2
	37 37	6 148.230	0.9	−0.8
	35 35	6 157.167	−4.7	−7.9
c-type transitions assigned with MWFTDR:				
3 1 3 3 0 3	11 11	4 945.840	−1.2	−12.2
4 985.547	9 9	5 033.503	−2.5	−11.7
	7 7	5 030.020	9.0	1.9
	5 5	4 987.699	−8.6	−14.1
	3 3	4 935.144	−0.8	−5.0
"forbidden"				
4 1 3 2 2 1	3* 3	12 204.685	−2.8	−25.6
11 775.783				

perturbed hyperfine components are of comparable magnitude.

Finally we performed a fit of only the coupling parameters to the differences of hyperfine components for an additional check. The values of the rotational and centrifugal distortion constants have been fixed to the values of Table 2a and the results are given in Table 4. The agreement is good in general and for all constants within the error limits.

In conclusion, the complex ground state microwave spectrum of isopropyl iodide could be mainly clarified. The high accuracy of the MWFT method in combination with the excellent agreement between experiment and the calculation method resulted in the determination of a set of highly precise molecular constants for isopropyl iodide including the spin rotation coupling parameters of iodine.

Table 2. Results from the simultaneous least squares fit analysis of the isopropyl iodide spectrum, A', B', C': rotational constants, D'_J, D'_{JK}, D'_K, δ'_J, R'_6: quartic centrifugal distortion constants of the van Eijck /Typke Hamiltonian [22, 23], $\chi_{gg'}$: quadrupole coupling constants ($\chi_- = \chi_{bb} - \chi_{cc}$), C_{gg}: spin rotation coupling constants, σ: total standard deviation, n: number of rotational transitions, N: number of hyperfine components. The components of the quadrupole coupling tensor in its own principal axis system (x', y', z') have been obtained by a rotation about the b-principal inertia axis with the angle α. Their errors have been calculated using the Gauss formula [25]. Standard errors are given in units of the last digits in parentheses. a): inclusion, b): exclusion of the iodine spin rotation coupling.

	a)	b)	
A'	8022.2104 (9)	8022.217 (3)	MHz
B'	2187.19215 (8)	2187.1913 (3)	MHz
C'	1817.66092 (8)	1817.6600 (3)	MHz
D'_J	0.400 (1)	0.392 (5)	kHz
D'_{JK}	1.926 (7)	1.90 (3)	kHz
D'_K	4.7 (1)	4.0 (5)	kHz
δ'_J	0.07705 (9)	0.0773 (4)	kHz
R'_6	−0.01428 (7)	−0.0137 (3)	kHz
χ_{aa}	−1626.155 (5)	−1626.17 (2)	MHz
χ_-	141.669 (5)	141.66 (2)	MHz
χ_{ac}	534.92 (1)	534.92 (5)	MHz
C_{aa}	3.2 (4)	–	kHz
C_{bb}	7.3 (1)	–	kHz
C_{cc}	6.8 (1)	–	kHz
σ:	3.3	13.1	kHz
n:	39	39	
N:	212	212	
Correlation coefficients co(X, Y) > |0.9|:			
co(B', C')	0.92	0.92	
co(C_{bb}, C_{cc})	0.91	–	
χ_{aa}	−1626.155 (5)	−1626.17 (2)	MHz
χ_{bb}	883.912 (3)	883.92 (1)	MHz
χ_{cc}	742.243 (3)	742.25 (1)	MHz
$\chi_{x'x'}$	883.912 (3)	883.92 (1)	MHz
$\chi_{y'y'}$	857.456 (6)	857.47 (2)	MHz
$\chi_{z'z'}$	−1741.368 (7)	−1741.38 (3)	MHz
α	12.1524 (3)	12.152 (1)	(°)

Table 3. Results from simultaneous least squares fit analysis with reduced data sets. The explanation of the symbols is given in Table 2. – a) Fit without the MWFTDR measurements. b) Fit without the MWFTDR measurements and without the hyperfine components containing one of the levels marked with an asterisk in Table 1. c) Like b) but with inclusion of the MWFTDR measurements (without the "forbidden" line).

	a)	b)	c)	
A'	8022.210 (1)	8022.215 (4)	8022.210 (1)	MHz
B'	2187.19216 (8)	2187.19218 (8)	2187.19215 (8)	MHz
C'	1817.66093 (8)	1817.66088 (8)	1817.66092 (8)	MHz
D'_J	0.400 (1)	0.399 (1)	0.399 (1)	kHz
D'_{JK}	1.926 (7)	1.926 (7)	1.929 (7)	kHz
D'_K	4.8 (1)	4.3 (4)	4.7 (2)	kHz
δ'_J	0.07703 (9)	0.0773 (2)	0.0771 (1)	kHz
R'_6	−0.01430 (9)	−0.0140 (3)	−0.0143 (1)	kHz
χ_{aa}	−1626.156 (5)	−1626.156 (5)	−1626.156 (5)	MHz
χ_-	141.668 (5)	141.668 (5)	141.669 (5)	MHz
χ_{ac}	534.93 (1)	534.99 (3)	534.98 (3)	MHz
C_{aa}	3.2 (4)	3.2 (4)	3.2 (4)	kHz
C_{bb}	7.3 (1)	7.3 (1)	7.3 (1)	kHz
C_{cc}	6.8 (1)	6.8 (1)	6.8 (1)	kHz
σ:	3.2	3.2	3.3	kHz
n:	37	37	38	
N:	206	200	205	
Correlation coefficients co(X, Y) > |0.9|:				
co(B', C')	0.92		0.91	
co(C_{bb}, C_{cc})	0.91	0.91	0.91	
co(A', D'_K)		−0.93		
co(A', δ'_J)		−0.91		
co(A', R'_6)		0.96		
co(δ'_J, D'_K)		0.94		
co(R'_6, D'_K)		−0.97		
co(R'_6, δ'_J)		−0.96		

Table 4. Results from the analysis of the hyperfine component differences. The components with the largest F-quantum numbers have been used as references. The values of the other spectroscopic constants have been fixed to those of Table 2a. N: Number of hyperfine component differences. The explanation of the other symbols is given in Table 2.

χ_{aa}	−1626.159 (6)	MHz	σ: 4.4 kHz
χ_-	141.674 (5)	MHz	n: 38
χ_{ac}	534.93 (2)	MHz	N: 173
C_{aa}	2.5 (4)	kHz	
C_{bb}	7.3 (1)	kHz	
C_{cc}	6.9 (1)	kHz	
Correlation coefficients co(X, Y) > |0.9|:			
co(C_{bb}, C_{cc})	0.94		

Acknowledgements

We thank the members of our group for help and discussions. We especially thank Prof. Dr. M.C.L. Gerry who was our guest in 1989 and has proposed the employed analyzing method. The funds were provided by the Deutsche Forschungsgemeinschaft, the Fond der Chemie and the Land Schleswig Holstein. The calculations were carried out at the computer center of the University of Kiel using mainly their new Cray-XMP 216 vector processor system.

[1] H. M. Jemson, W. Lewis-Bevan, N. P. C. Westwood, and M. C. L. Gerry, J. Mol. Spectrosc. **119,** 22 (1986).
[2] D. T. Cramb, M. C. L. Gerry, and W. Lewis-Bevan, J. Chem. Phys. **88,** 3497 (1988).
[3] J. Gripp, Dissertation, Universität Kiel 1989.
[4] P. Groner, Y. S. Li, and J. R. Durig, J. Mol. Spectrosc. **72,** 20 (1978).
[5] C. Ikeda, T. Inagusa, and M. Hayashi, J. Mol. Spectrosc. **135,** 334 (1989).
[6] W. Stahl, J. Gripp, N. Heineking, and H. Dreizler, Z. Naturforsch. **42a,** 392 (1987).
[7] J. Gripp, H. Dreizler, J. Gadhi, G.Wlodarczak, J. Legrand, J. Burie, and J. Demaison, J. Mol. Spectrosc. **129,** 381 (1988).
[8] J. Gripp and H. Dreizler, Z. Naturforsch. **43a,** 971 (1988).
[9] G. Bestmann, H. Dreizler, H. Mäder, and U. Andresen, Z. Naturforsch. **35a,** 392 (1980).
[10] G. Bestmann and H. Dreizler, Z. Naturforsch. **37a,** 58 (1982).
[11] G. Bestmann, H. Dreizler, E. Fliege, and W. Stahl, J. Mol. Struct. **97,** 215 (1983).
[12] W. Stahl, G. Bestmann, H. Dreizler, U. Andresen, and R. Schwarz, Rev. Sci. Instrum. **56** (9), 1759 (1985).
[13] H. Dreizler, U. Andresen, J. Gripp, I. Merke, M. Meyer, W. Stahl, R. Schwarz, and K. Vormann, Z. Naturforsch. **42a,** 1279 (1987).
[14] Ch. Keussen, N. Heineking, and H. Dreizler, Z. Naturforsch. **44a,** 215 (1989).
[15] H. Ehrlichmann, J. U. Grabow, H. Dreizler, N. Heineking, R. Schwarz, and U. Andresen, Z. Naturforsch. **44a,** 751 (1989).
[16] W. Gordy and R. L. Cook, Microwave Molecular Spectra, J. Wiley, New York 1984, p. 426f.
[17] A. R. Edmonds, Drehimpulse in der Quantenmechanik, BI Hochschultaschenbücher, Mannheim 1964, p. 59f., p. 112f.
[18] Loc. cit. [3].
[19] G. W. King, R. M. Hainer, and P. C. Cross, J. Chem. Phys. **11,** 27 (1943).
[20] Loc. cit. [16], p. 469.
[21] J. Haekel and H. Mäder, Z. Naturforsch. **43a,** 203 (1988).
[22] B. P. van Eijck, J. Mol. Spectrosc. **53,** 246 (1974).
[23] V. Typke, J. Mol. Spectrosc. **63,** 170 (1976).
[24] Loc. cit. [16], p. 418ff.
[25] E. Fliege, Dissertation, Universität Kiel 1989.